https://doi.org/10.5194/egusphere-2025-6301
Preprint. Discussion started: 1 April 2026

Antarctic Sea Ice Variations and Their Linkages with Global Extreme Weather Events

Shulin Tang[a,b], **Yaozong Zhang**[a,b]

[a] School of Geography and Planning, Longdong University, Qingyang 745000, Gansu, China

[b] Qingyang Tech Innovation Center of Remote Sensing on Soil and Water Conservation and Desertification Control, Longdong University, Qingyang 745000, Gansu, China

Corresponding Author: Shulin Tang; Email: tangshulin@126.com

Abstract

Antarctic sea ice is a critical indicator of global climate dynamics, yet its post-2015 accelerated retreat and links to extreme weather/key climate modes remain insufficiently characterized. To address these gaps, we analyse 2010–2024 multi-source data (NSIDC sea ice extent (SIE), CMA extreme weather records, NOAA ENSO indices) via spatiotemporal decomposition, non-linear modelling, and mechanistic dissection. Antarctic SIE showed a "stable-then-decline" trend: minimal variability 2010–2014 (peak: 20.16×10^6 km², Sep 2014), followed by unprecedented post-2015 retreat to a Feb 2023 historic minimum (1.85×10^6 km², ~20% below 2010–2014 summer mean). The Amundsen–Bellingshausen Sea and Antarctic Peninsula were main retreat zones, with 2020–2024 declines (10–15%/20–25% winter/summer) exceeding East Antarctica (5–10%) and Ross Sea (8–12%). We identified tiered negative covariance between SIE and extreme weather, presumably co-modulated by the El Niño-Southern Oscillation (ENSO) and Southern Annular Mode (SAM): strong associations ($R^2 \geq 0.6$, $P < 0.001$) for extreme heat (400% frequency increase) and cold waves (700% increase), potentially via albedo–circulation feedback; moderate associations ($0.5 \leq R^2 < 0.6$, $0.001 \leq P < 0.01$) for floods/rainstorm/typhoons, likely from ACC heat transport changes and convective propagation; weak associations ($R^2 < 0.4$, $P \approx 0.05$) for blizzards, possibly due to spatially constrained El Niño–SAM effects. La Niña-positive SAM may have amplified these linkages (e.g., 400% extreme heat increase in 2021–2023 triple La Niña), while El Niño-negative SAM suppressed them. These findings advance polar-low latitude coupling understanding, aiding extreme weather prediction and IPCC AR6-aligned adaptation.

Keywords: Antarctic Sea Ice Extent; Global Extreme Weather; ENSO; Southern Annular Mode; Climate Correlation

1 Introduction

Antarctic sea ice, as a key regulator of the Earth's climate system, profoundly influences global energy balance and ocean circulation patterns by governing heat, momentum, freshwater, and gas exchange between the atmosphere and ocean (Morioka et al., 2024; Zhu et al., 2023). Climate coupled models predict that sea ice melt will cause localized surface warming, which propagates to the global troposphere via the 'polar amplification effect' (Tewari et al., 2023). Satellite observations from 1979 to 2024 reveal a phased abrupt change in Antarctic sea ice: a slight increase from 1979 to 2012 (Parkinson, 2019), followed by unprecedented rapid retreat after 2015, with successive record lows

https://doi.org/10.5194/egusphere-2025-6301
Preprint. Discussion started: 1 April 2026

occurring in February 2022 and the winter of 2023. Notably, the SIE in February 2023 reached a low of 1.85 million km², representing a reduction of approximately 20% compared to the 2010–2014 summer mean, with a retreat rate significantly exceeding that of Arctic Sea ice (Purich & Doddridge, 2023; Diamond et al., 2024). This 'initial expansion followed by contraction' pattern defies traditional climate model predictions, highlighting the Antarctic sea ice's high sensitivity to global climate change.

Spatially, Antarctic sea ice retreat is not uniform: during 2020–2024, the 'core retreat zones' encompassed the western Antarctic (Amundsen–Bellingshausen Sea) and the Antarctic Peninsula periphery. Winter sea ice concentration in these areas decreased by 10–15% compared to 2010–2019, and summer decline by 20–25%, significantly exceeding the retreat rates observed in the East Antarctic (5–10%) and Ross Sea (8–12%) (Josey et al., 2024; Cordero et al., 2023). This regional differentiation reflects both the synergistic interaction between local ocean circulation (such as the Antarctic Circumpolar Current (ACC)) and atmospheric processes, and suggests that sea ice changes may exert spatially differentiated impacts on climate systems at different latitudes (Wang et al., 2021)

Amidst the dramatic changes in Antarctic Sea ice, extreme weather events worldwide are exhibiting a trend of increasing frequency and intensity (Intergovernmental Panel on Climate Change [IPCC], 2022). Observational data indicate that the frequency of global extreme heat events in 2024 increased by 37% compared to the 2010–2020 average, with 2024 surpassing 2023 to become the hottest year on record (Jha et al., 2025). Regional extreme events have also intensified. For instance, during the winter of 2023, the number of storm days in the northern Weddell Sea and northwestern Ross Sea increased by 7 days per month compared to the 1990–2015 average, with the northern Weddell Sea rising from 9.1 days to 11.6 days (Josey et al., 2024). By event type, the intensity and frequency of extreme heat, rainstorm, and typhoons/storms have significantly increased (Chen et al., 2023). Meanwhile, extreme cold events remain more frequent and difficult to predict under global warming (He et al., 2019). Between 2010 and 2024, the annual frequency of these extreme events significantly exceeded the 1981–2010 baseline period, with further increases observed from 2021 to 2024, underscoring the severity of global extreme climate conditions.

Existing research confirms a link between Antarctic sea ice changes and global extreme weather events: sea ice retreat alters polar albedo and the phase of the SAM, triggering anomalies in mid-to-low-latitude atmospheric circulation (such as increased north-south oscillation of the westerly jet stream). This, in turn, modulates the environmental conditions conducive to extreme event generation (Bader et al., 2012; Eabry et al., 2024; Cordero et al., 2023). For instance, Zhu et al. (2023) numerically simulated that a 10% reduction in Antarctic sea ice correlates with an 8–12% increase in mid-to-low-latitude extreme precipitation events; Josey et al. (2024) observed that during the record-low SIE in 2023, when tropical western Pacific sea surface temperature anomalies reached +1.5°C, typhoon generation frequency increased by 40% compared to the long-term average. However, current research still faces three core gaps: first, insufficient quantitative characterization of the relationship between multi-scale sea ice evolution (particularly decadal variability) and extreme events; existing studies predominantly focus on qualitative trends at the global scale, lacking hierarchical analyses of the strength of associations between different types of extreme events (such as heatwaves, cold spells, and typhoons) and sea ice indicators (SIE). Furthermore, the identification of key influence periods (such as the spring SAM positive phase) remains unclear (Cordero et al., 2023). Second, the climate mode modulation mechanism remains unresolved (Morioka et al., 2024; Dou et al., 2022).

As key Southern Hemisphere climate modes, El Niño–Southern Oscillation (ENSO) and SAM (Wang

https://doi.org/10.5194/egusphere-2025-6301
Preprint. Discussion started: 1 April 2026

et al., 2023) exert regulatory influence on sea ice-extreme event linkages, though their precise pathways remain contentious — for instance, El Niño years may locally increase Ross Sea sea ice via Rossby wave teleconnections, temporarily weakening the negative correlation between sea ice and extreme heat (Zhang et al., 2021), while La Niña years may amplify sea ice retreat trends (Wang et al., 2025). However, the specific impacts of both on regional-scale extreme events (such as the West Antarctic rainstorm) remain unquantified; Thirdly, observational and modelling constraints limit research depth: at the observational level, Antarctic sea ice data suffers from 'marginal zone uncertainty'—satellite sensors (such as SMMR and SSMIS) exhibit insufficient identification accuracy for areas with sea ice concentration below 15%, leading to biases in the National Snow and Ice Data Center (NSIDC) data for marginal seas like the Antarctic Peninsula (Crosta et al., 2021); At the modelling level, while CMIP6 climate models (e.g., CanESM5, CESM2) can simulate the overall negative correlation between sea ice and extreme climate events, they inadequately capture the abrupt retreat events post-2016. Furthermore, their relatively low resolution (typically 1°×1°) hinders accurate characterisation of interactions between deep convection in the Southern Ocean and sea ice (Heuzé et al., 2021; Morioka et al., 2024). Furthermore, existing research has paid scant attention to regional extreme climate responses in areas adjacent to Antarctica (such as the West Antarctic Peninsula and Ross Sea), hindering the formulation of regional-scale climate adaptation strategies.

This study integrates multi-source data from 2010 to 2024 (NSIDC sea ice data, China National Climate Centre extreme event data, NOAA ENSO indices) within an observational-simulation-mechanism three-dimensional analytical framework. It aims to achieve three core objectives: (1) To characterize the spatiotemporal evolution of Antarctic SIE from 2010 to 2024, **laying the foundation for linkage analysis**; (2) to quantify the strength of associations between different types of extreme climate events and sea ice indicators, identifying key sensitive regions and time periods; (3) to elucidate the **potential** modulation mechanisms of ENSO and SAM on the sea ice–extreme event linkage. The findings offer new insights into the coupling mechanisms between polar and low-latitude climates, the interannual variability of sea ice, and extreme weather events. They provide scientific support for global extreme event forecasting and early warning systems, as well as for regional climate adaptation strategies in line with the IPCC Sixth Assessment Report (AR6).

2 Data and Methods

Data Sources:

SIE and selected sea ice concentration (SIC) data for 2010–2024 are sourced from NSIDC (Fetterer et al., 2017).

Data on major global weather and climate disaster events are based on monthly releases from the China National Climate Centre (2010–2024), covering occurrence times, locations, and intensity information for global extreme heatwaves, extreme rainfall events, floods, typhoons/storms, cold waves, heavy snowfall, and tornadoes.

Monthly Niño Eastern Pacific Index (NEPI) and Niño Central Pacific Index (NCPI) for 2010–2024 are sourced from the Global Ocean Data Assimilation System (GODAS; Behringer & Xue, 2004), provided by the National Centers for Environmental Prediction (NCEP) of the U.S. National Oceanic and Atmospheric Administration (NOAA). The data cover latitudes 75°S–65°N with a horizontal

https://doi.org/10.5194/egusphere-2025-6301
Preprint. Discussion started: 1 April 2026

resolution of 1°×1°.

Data processing:

Using the median SIE values for 1981–2010 as the baseline, daily SIE data from 2010 to 2024 were employed to calculate annual SIE daily anomalies for this period according to Equation (1).

$$SIE_{DN} = \frac{SIE_X - SIE_A}{SIE_A} \times 100\% \quad (1)$$

Where: SIE_{DN} — Daily Anomaly of SIE (%); SIE_X — Known daily SIE (Unit: Millions km²); SIE_A — Daily average SIE from 1981 to 2010 (Unit: Millions km²)

After obtaining the SIE_{DN} values, the annual average SIE anomaly (SIE_{YN}) from 2010 to 2024 was calculated using Equation (2).

$$\overline{SIE_{YN}} = \frac{1}{n}\sum_{i=1}^{n} SIE_{DN}i \quad (2)$$

Where: SIE_{YN} — Annual average *SIE* anomaly

The annual average SIE (SIE_Y) was obtained using Equation (3)

$$\overline{SIE_Y} = \frac{1}{n}\sum_{i=1}^{n} SIE_D i \quad (3)$$

Where: SIE_Y — Annual average *SIE;* SIE_D — Daily *SIE*

In selecting and statistically analysing major hazardous weather and climate events, this study focuses on seven primary categories of hazardous events globally between 2010 and 2024: extreme heat, torrential rainfall, flooding, typhoons/storms, tornadoes, blizzards, and cold waves. Event samples are sourced from the monthly monitoring reports titled "Global Major Hazardous Weather and Climate Events" issued by the National Climate Centre of China. The study systematically collated the annual occurrence frequency of each event type over the 15-year period, plotting time series graphs and trend lines to reveal their interannual variation characteristics.

The correlation analysis between global extreme climate events and Antarctic SIE employed an exponential regression model (Osborne, 2010). This model better accommodates the nonlinear characteristics of the climate system, where "small perturbations trigger large responses" — for instance, a modest reduction in Antarctic sea ice may precipitate an accelerated increase in the frequency of extreme events.

$$ln(Y) = \beta_1 X + \beta_0 \quad (4)$$

$$Y = exp(\beta_1 X + \beta_0) = exp(\beta_0) \bullet exp(\beta_1 X) \quad (5)$$

Where: β_0 — Intercept, corresponding to the intercept of the linear relationship between $ln(Y)$ and X in the figure; β_1 — Slope; Y — Frequency of extreme weather and climate events; X — SIE.

3 Results and Discussion

https://doi.org/10.5194/egusphere-2025-6301
Preprint. Discussion started: 1 April 2026

3.1 Spatiotemporal Characteristics of Antarctic Sea Ice from 2010 to 2024

Antarctic SIE from 2010 to 2024 exhibits pronounced seasonal fluctuations and long-term trends (Figure 1). Within each year, it follows a pattern of increasing during winter and decreasing during summer, peaking at 17–18 million km² in September (Southern Hemisphere winter) and reaching a trough of 2–3 million km² in February (Southern Hemisphere summer). Interannual variations exhibit a "stable-then-declining" pattern. Between 2010 and 2014, SIE fluctuations were minor (±0.3 million km²), with the period's peak recorded on 21 September 2014 (20.16 million km²). After 2015, SIE commenced a marked decline, with the period 2020–2024 marking the most dramatic Antarctic sea ice changes since 2010. Winter peaks fell to 17–17.5 million km², while the summer SIE annual mean (2.2 million km²) decreased by 15.4% compared to the 2010–2019 average (2.6 million km²), and interannual variability expanded to ±0.4 million km². Furthermore, summer minima below 2 million km² occurred consecutively in 2022 and 2023, with a record minimum of 1.85 million km² recorded on 21 February 2023—approximately 20% below the 2010–2014 summer mean. This aligns with the

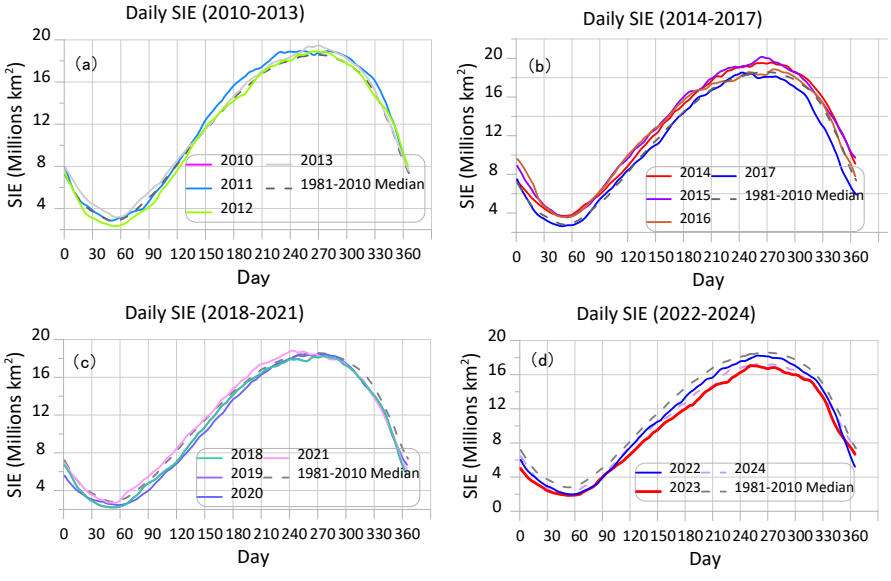

Figure 1. Antarctic sea ice daily extent from 2010 to 2024.
Note: This figure shows the daily variations in Antarctic SIE from 2010 to July 2024. Subfigures a–d display the median daily SIE for the period 1981–2010, indicated by gray dashed lines. Each panel presents SIE changes during specific time periods (colored solid lines): (a) 2010–2013; (b) 2014–2017; (c) 2018–2021; (d) 2021–2024.

record-low SIE values reported by Josey et al. (2024) for 2023. Evidently, the SIE in 2023 and similar years lies markedly below historical median levels, showing a trend toward converging with historical lows.

From a spatial distribution perspective, Antarctic sea ice variations exhibit pronounced regional differences and heterogeneity. Spatial characteristics during extreme years present stark contrasts (Figure 2): In September 2014 (a high-sea-ice year), areas with 80–100% high-density sea ice were

https://doi.org/10.5194/egusphere-2025-6301
Preprint. Discussion started: 1 April 2026

concentrated in the Indian Ocean sector and the Weddell Sea, with the sea-ice edge lying 1–2 latitudes beyond the median of the 1981–2010 baseline period. In February 2023 (a low-sea-ice year), high-density areas contracted substantially, persisting only in the western Ross Sea along the Antarctic coast, parts of the Amundsen Sea, and Prydz Bay in East Antarctica—sea-ice density in the Indian Ocean sector dropped to 50–70%, while ice near the southern tip of South America nearly vanished. The sea-ice edge retreated 5–8 degrees of latitude toward the Antarctic continent compared to September 2014, with the most pronounced retreat occurring in the Atlantic–Indian Ocean sector between 60°W and 60°E longitude. This retreat was the primary driver of the low SIE during that summer. Concurrently, during 2020–2024, the southwestern Antarctic (Amundsen–Bellingshausen Seas) and the periphery of the Antarctic Peninsula emerged as 'core zones' for sea ice retreat: Winter sea ice concentration in this region decreased by 10–15% compared to the 2010–2019 period, while summer concentration declined by 20–25%. These rates significantly exceeded those observed in East Antarctica (5–10%) and the Ross Sea (8–12%), further highlighting the spatial heterogeneity of Antarctic sea ice changes.

The retreating period under study in this research may have been influenced by different controlling factors compared to the earlier expansion period (1979–2014), and further verification with a longer time series is required.

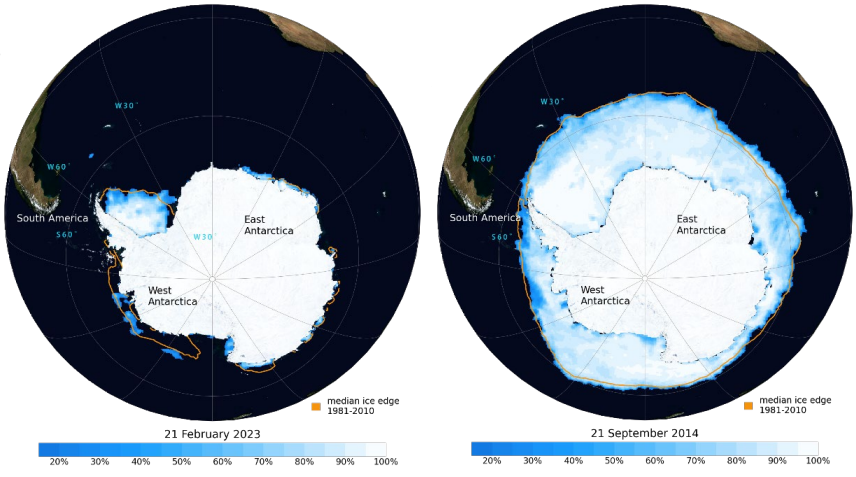

Figure 2. Sea Ice Concentration Corresponding to Maximum and Minimum SIE (2010–2024). The orange dashed line represents the 1981–2010 average SIE. (Left: Lowest SIE on February 21, 2023; Right: Highest SIE on September 21, 2014)

3.2 Quantification of Dynamic Linkages Between Global Extreme Events and Antarctic SIE (2010–2024)

Building upon the aforementioned spatiotemporal characteristics of sea ice—established to support the core goal of exploring sea ice-extreme weather connections—this section undertakes a quantitative analysis of the dynamic associations between Antarctic SIE and global extreme climate events.

During the period 2010–2024, SIE exhibited an overall declining trend. As a key regulator within the global climate system, the reduction in SIE directly influences the frequency and intensity of extreme weather events (Cvijanovic et al., 2015). This reduction further strengthens the correlation with

https://doi.org/10.5194/egusphere-2025-6301
Preprint. Discussion started: 1 April 2026

extreme events—the frequency of various extreme weather events increases as sea ice declines, although the degree of influence and statistical reliability varies significantly across different event types.

The dynamic relationship between the frequency of global extreme weather events and the Antarctic annual mean SIE from 2010 to 2024 is illustrated in Figure 3: the overall SIE, represented by the red dashed line, exhibits a fluctuating downward trend, while the frequency of various extreme weather events generally increases to varying degrees as SIE declines. Specifically, in 2010, when SIE levels were relatively high, the frequency of extreme heat events was low; however, following a marked decline in SIE after 2020, the frequency of extreme heat events increased significantly. Patterns for torrential rain, floods, typhoons/storms, cold waves, and tornadoes mirrored those of extreme heat, with marked increases during periods of low SIE; while heavy snowfall frequency showed some increase during SIE decline, its visual correlation with SIE was comparatively weaker than that of other events.

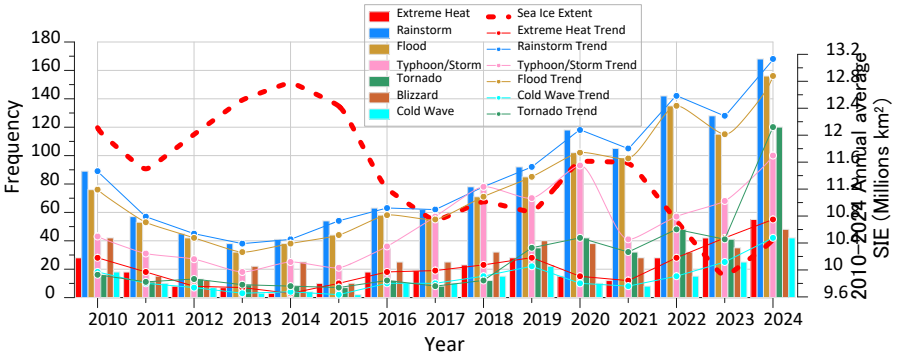

Figure 3. Relationship between the Frequency of Global Extreme Climate Events and the Annual Average SIE. Note: The horizontal axis represents the year (2010–2024); the left vertical axis represents the frequency of extreme climate events (Unit: times); the right vertical axis represents the annual average Antarctic SIE (in million km²). Bar charts of different colors represent different types of extreme events: red for extreme high temperatures, blue for rainstorms, orange for typhoons/storms, purple for cold waves, and gray for blizzards. The red dashed line represents the trend of SIE change from 2010 to 2024.

Through exponential fitting analysis of extreme events and SIE data from 2010 to 2024 (Figures 4a–g), combined with the decreasing trend of SIE and statistically significant P-values (typically using $P < 0.05$ as the significance threshold), the association between extreme events and SIE can be categorized into four types. The response intensity and statistical reliability vary significantly across these categories, all reflecting the core pattern that "decreasing SIE leads to increased frequency of extreme events."

Sea ice retreat exerts a significant driving effect on the increased frequency of extreme heatwaves and cold spells. Regression analysis indicates that when the annual mean SIE decreased from approximately 12.8 million km² (high value) to 9.6 million km² (low value), the frequency of extreme heat events increased from approximately 10 events per year to approximately 50 events per year, representing a cumulative increase of 400%. The exponential fit correlation between the two variables

https://doi.org/10.5194/egusphere-2025-6301
Preprint. Discussion started: 1 April 2026

was highly significant (R^2 = 0.722, P < 0.0001) (Figure 4a). Concurrently, cold wave frequency increased from approximately 5 events per year to around 40 events per year, representing a 700% rise, with a similarly highly significant correlation with SIE (R^2 = 0.643, P = 0.0014) (Figure 4f). These findings indicate that the reduction in SIE is likely a significant driver behind the significant increase in the frequency of extreme heat and cold wave events.

3.2.1 Strongly negative and highly significant association ($R^2 \geq 0.6$, $P < 0.001$):

Sea ice retreat exerts a significant driving effect on the increased frequency of extreme heatwaves and cold spells. Regression analysis indicates that when the annual mean SIE decreased from approximately 12.8 million km² (high value) to 9.6 million km² (low value), the frequency of extreme heat events increased from approximately 10 events per year to approximately 50 events per year, representing a cumulative increase of 400%. The exponential fit correlation between the two variables

was highly significant (R^2 = 0.722, P < 0.0001) (Figure 4a). Concurrently, cold wave frequency increased from approximately 5 events per year to around 40 events per year, representing a 700% rise, with a similarly highly significant correlation with SIE (R^2 = 0.663, P = 0.000221) (Figure 4b). These findings indicate that the reduction in SIE is likely a significant driver behind the significant increase in the frequency of extreme heat and cold wave events.

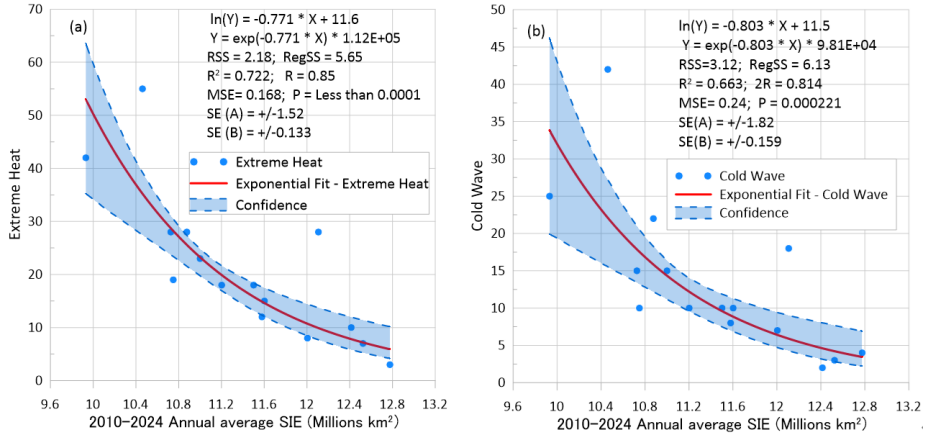

Figure 4. Relationship between Annual Average SIE and Frequency of Extreme Heat Events (a) and Cold Waves (b), 2010–2024. Note: The blue scatter points represent actual event frequencies for each year, red curves indicate the exponential fit, and blue shaded areas denote confidence intervals. Statistical metrics—including the fitted equation, coefficient of determination (R^2), mean squared error (MSE), and p-value—are provided to reflect the strength and significance of the association.

3.2.2 Strong Negative Correlation with Statistical Significance ($0.5 \leqslant R^2 < 0.6$, $0.001 \leqslant P < 0.01$)

Floods, rainstorms, and typhoons/storms fall into this category (Fig 5). A clear association exists between declining annual average SIE values and increased frequency of these events, though the correlation strength is weaker than that of strongly correlated events, potentially influenced by

https://doi.org/10.5194/egusphere-2025-6301
Preprint. Discussion started: 1 April 2026

atmospheric circulation and precipitation distribution factors. Sea ice retreat also exerts a driving effect on the increased frequency of floods, rainstorm, and typhoons/storms. Furthermore, the correlation characteristics between different extreme events and sea ice indicators exhibit variations.

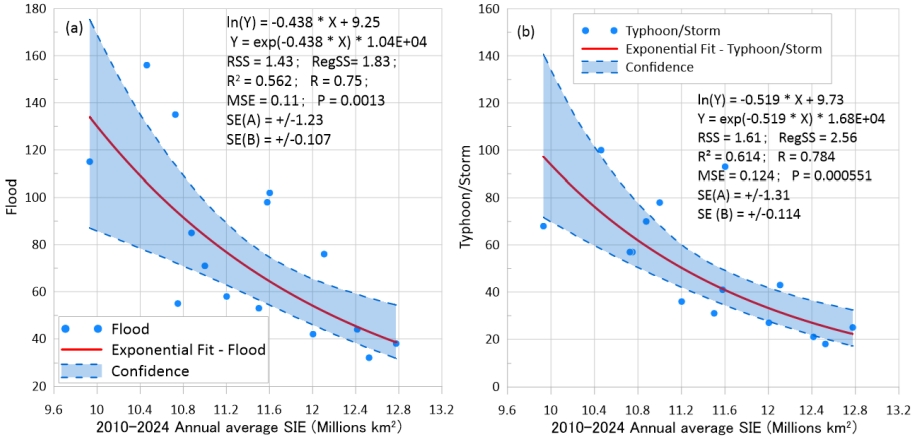

From the SIE perspective, when the annual average SIE decreased from approximately 12.8 million km² (high value) to 9.6 million km² (low value): flood frequency increased from about 40 events/year to approximately 160 events/year, representing a 300% increase, with a significant fitted relationship ($R^2 = 0.562$, $P = 0.0013$) (Figure 5a); the frequency of rainstormevents increased from approximately 20 events per year to about 100 events per year, representing a 400% increase, with the correlation remaining statistically significant ($R^2 = 0.533$, $P = 0.00198$) (Figure 5c); typhoon/storm frequency increased from approximately 20 events per year to about 80 events per year, representing a 300% increase, with a stronger correlation ($R^2 = 0.614$, $P = 0.000551$) (Figure 5b). This indicates that sea ice retreat exerts a significant regulatory influence on the oceanic thermal and dynamic conditions essential for typhoon/storm formation (Josey et al., 2024).

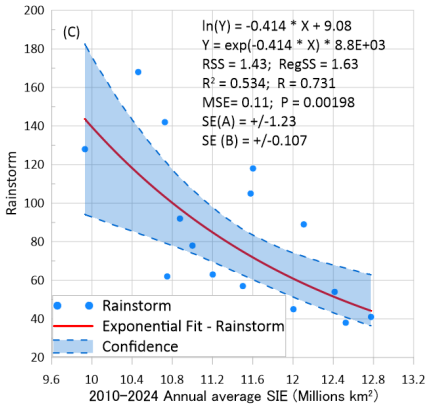

Figure 5. Relationship between Annual Average SIE and Frequency of Floods (a), Typhoons/Storms (b), and Rainstorms (c), 2010–2024. See Figure 4 for notes.

3.2.3 Moderately Negative and Significant Correlation Category ($0.3 \leq R^2 < 0.5$, $0.01 \leq P < 0.05$)

The association strength between the occurrence frequency of blizzards and tornadoes and the Antarctic annual average SIE is relatively weak (Fig 6). Their variations are more influenced by local climatic conditions, observational methods, and regional environmental factors, exhibiting only a

https://doi.org/10.5194/egusphere-2025-6301
Preprint. Discussion started: 1 April 2026

weak overall trend. Although sea ice retreat contributes to increased frequencies of blizzards and tornadoes, their statistical correlation with sea ice indicators is markedly weaker compared to extreme events such as floods, rainstorm, and typhoons/storms. This suggests that their variability may be predominantly driven by non-sea-ice factors. Specifically, when the annual average SIE decreased from 12.8 million km² (high value) to 9.6 million km² (low value): the frequency of blizzards increased from approximately 10 events per year to 40 events per year—a 300% increase—but its relationship with SIE was weakly fitted ($R^2 = 0.266$, $P = 0.0492$) (Figure 6a); tornado frequency increased from approximately 20 events per year to 100 events per year, representing a 400% increase. Its association

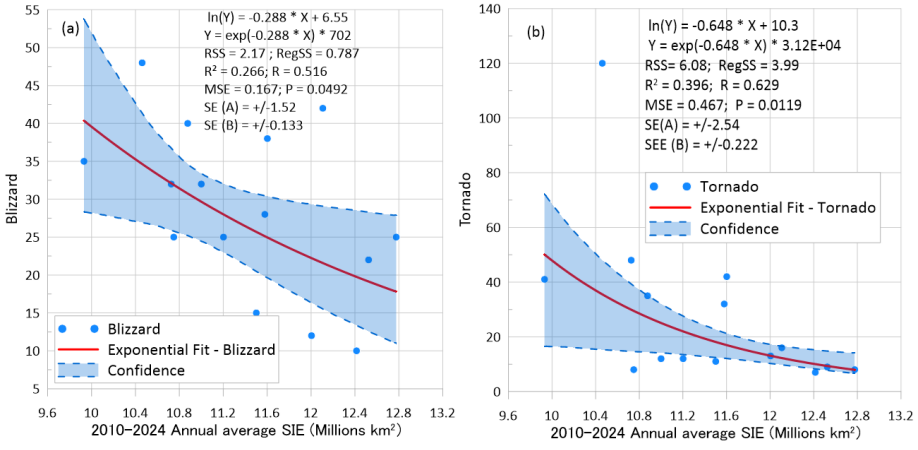

Figure 6. Relationship between Annual Average SIE and Frequency of blizzards (a) and tornadoes (b), 2010–2024. See Figure 4 for notes.

with SIE was slightly stronger than that of blizzards ($R^2 = 0.396$, $P = 0.0119$) (Figure 6b), though still at a relatively low level. Furthermore, tornado frequency changes are more likely regulated by regional dynamic processes such as atmospheric vertical wind shear and topography, with sea ice retreat not being a core driving mechanism.

Comprehensive analysis of 2010–2024 data reveals a significant decreasing trend in Antarctic SIE, while the frequency of extreme heat, rainstorm, floods, typhoons/storms, blizzards, cold waves, and tornadoes has generally increased, showing a significant negative correlation between the two. In terms of statistical significance, extreme heat, cold waves, typhoons/storms, floods, and rainstormall exhibit significant correlations at $P < 0.05$. The intensity of response follows this order: extreme heat > cold waves > typhoons/storms > floods > rainstorm> tornadoes > blizzards.

3.3 Discussion on Correlation Mechanisms

Correlation and Influence Pathways Between Antarctic SIE Anomalies, ENSO, and the Extreme Events: Comparing Antarctic SIE anomalies from 2010 to 2024 with concurrent ENSO indices (NEPI index, NCPI index) and different types of extreme events reveals that during significant El Niño years (e.g., 2010, 2013–2015), both the NEPI index (Figure 7a) and the NCPI index (Figure 7b) exceed 0, corresponding to positive SIE anomalies (Figure 7c) during the same periods, indicating increased SIE. Conversely, during La Niña years (e.g., 2011, 2017, 2018, and 2021–2023), both the NEPI and the

https://doi.org/10.5194/egusphere-2025-6301
Preprint. Discussion started: 1 April 2026

NCPI indices were below zero, corresponding to negative SIE anomalies during these periods. Notably, the "Triple La Niña" event from 2021 to 2023 exhibited significantly negative SIE anomalies, and the occurrence and frequency of various extreme events also show corresponding relationships with these ENSO phases and SIE anomalies (Figure7d).

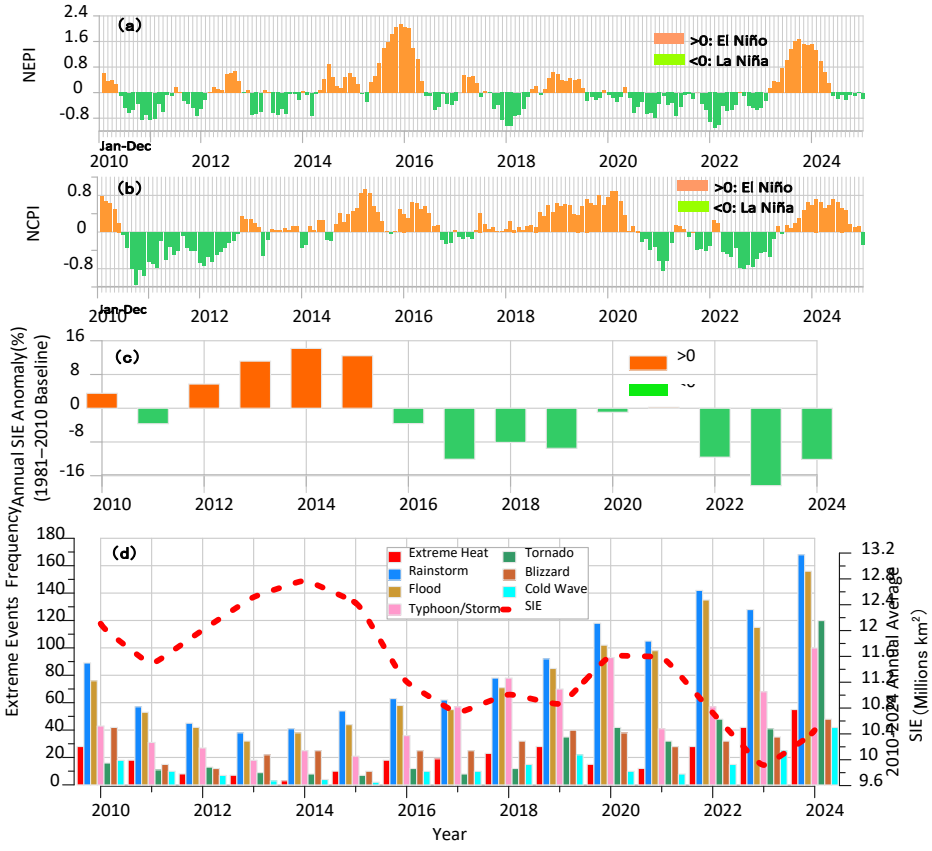

Figure 7. Relationships among El Niño, La Niña, Global Extreme Weather Events, and Antarctic SIE Variations from 2010 to 2024.

Note: This figure displays indices related to El Niño and La Niña events in 2010–2024, as well as changes in the frequency of global extreme weather events and Antarctic SIE. (a) NEPI; (b) NCPI. Orange areas signify that the corresponding indices are greater than 0, representing El Niño events; green areas signify that the corresponding indices are less than 0, representing La Niña events. (c) The red dashed line represents the annual average extent of Antarctic sea ice. The orange bar chart indicates cases where the anomaly percentage based on the median Sea Ice Extent (SIE) from 1981 to 2010 is greater than 0, while the green bar chart indicates cases where this anomaly percentage is less than 0. (d) Bar charts of different colors respectively represent the occurrence frequencies of Extreme Heat, Rainstorm, Flood, Typhoon/Storm, Tornado, Blizzard, and Cold Wave. The red dashed line indicates the Antarctic SIE.

Regarding the influencing mechanisms, different ENSO phases can exert differential impacts on Antarctic SIE through anomalous atmospheric circulation (Dash et al., 2012; Gurjão et al., 2025), and these impacts may further relate to the generation and characteristics of extreme events: During El Niño years, anomalously elevated sea surface temperatures in the equatorial Pacific trigger a dominant

https://doi.org/10.5194/egusphere-2025-6301
Preprint. Discussion started: 1 April 2026

Rossby wave–dominated atmospheric teleconnection wave train. Upon propagating to Antarctica, this wave train alters local atmospheric circulation patterns. For instance, it induces anomalous easterly or southerly winds in certain Antarctic peripheral regions (e.g., the Ross Sea), promoting sea ice accumulation and persistence, thereby increasing local SIE (Dou & Zhang, 2022), which in turn may influence the occurrence conditions of extreme events in relevant regions. In contrast, during La Niña years, the equatorial Pacific experiences abnormal sea surface temperature cooling. Atmospheric circulation teleconnections transport more warm air to Antarctica, accelerating sea ice melt and resulting in reduced SIE (Wang et al., 2025), and such changes in sea ice and atmospheric circulation can also have implications for the frequency and intensity of extreme events.

The index regression analysis for 2010–2024 indicates that the association between Southern Ocean SIE and global extreme weather events exhibits a three-tiered differentiation of "strong–moderate–weak." Extreme heatwaves and cold waves show strong correlations with SIE, with a coefficient of determination $R^2 \geq 0.6$ and a significance level $P < 0.001$. Floods and typhoons/storms exhibit moderate associations, with R^2 between 0.5 and 0.6 and P values ranging from 0.001 to 0.01. Snowstorms and tornadoes show weak associations, characterized by $R^2 < 0.4$ and $P \approx 0.05$. This differentiation in correlation stems from the multi-layer coupling between sea ice, atmosphere, and ocean. It is simultaneously regulated by the synergistic interaction between the ENSO and the SAM phase, ultimately forming a systematic framework where "event type determines the core mechanism, while climate modes modulate the correlation strength (Figure 8)."

Extreme Heat: Sea ice retreat triggers a positive feedback loop of "albedo–warming–melt," with ENSO and SAM phases synergistically amplifying the correlation strength. Antarctic sea ice has an albedo of approximately 0.8; its retreat reduces surface albedo to ocean levels (around 0.1). During 2010–2024, every 10% decrease in Antarctic SIE increased polar solar radiation absorption by 15–20%, resulting in local warming of 2–3°C per decade (Zhu et al., 2023). This warming effect propagates through atmospheric circulation to mid- and low-latitudes, resulting in a 37% increase in global extreme heat frequency in 2024 compared to the 2010–2020 average (Jha et al., 2025; Ji et al., 2023), directly corresponding to a strong correlation with $R^2 = 0.722$ ($P < 0.0001$).

Additionally, sea ice retreat has reduced the temperature gradient in the mid-to-high latitudes of the Southern Hemisphere by 0.6–0.8°C (Chen et al., 2024), decreased atmospheric baroclinicity by 15% (Rantanen et al., 2018), and thereby expanded the north-south oscillation amplitude of the westerly jet stream from ±1.2° to ±2.0°. This accelerates the northward transport of warm air from low latitudes, extending the duration of high temperatures from 3–5 days to 7–10 days. Simultaneously, reduced sea ice inhibits deep oceanic convection in the Southern Ocean (Morioka et al., 2024), diminishing heat release from the ocean to the atmosphere and further stabilizing the high-temperature environment.

The 2021–2023 triple La Niña deepened the Antarctic Low (reducing central pressure by 5 hPa) through teleconnections, while the positive SAM phase (61% prevalence) amplified jet stream variability. Their combined effect increased summer heatwave frequency by 400% during 2020–2024 (Figure 5d). Conversely, El Niño stimulates Rossby waves, locally increasing SIE in the Ross Sea by 8–10% (Zhang et al., 2021). Additionally, the negative SAM phase stabilizes the westerly jet stream—during the 2015 El Niño event, high-temperature frequency dropped to only 10 occurrences (the lowest in the study period), with the correlation strength between the two factors decreasing by 30%.

https://doi.org/10.5194/egusphere-2025-6301
Preprint. Discussion started: 1 April 2026

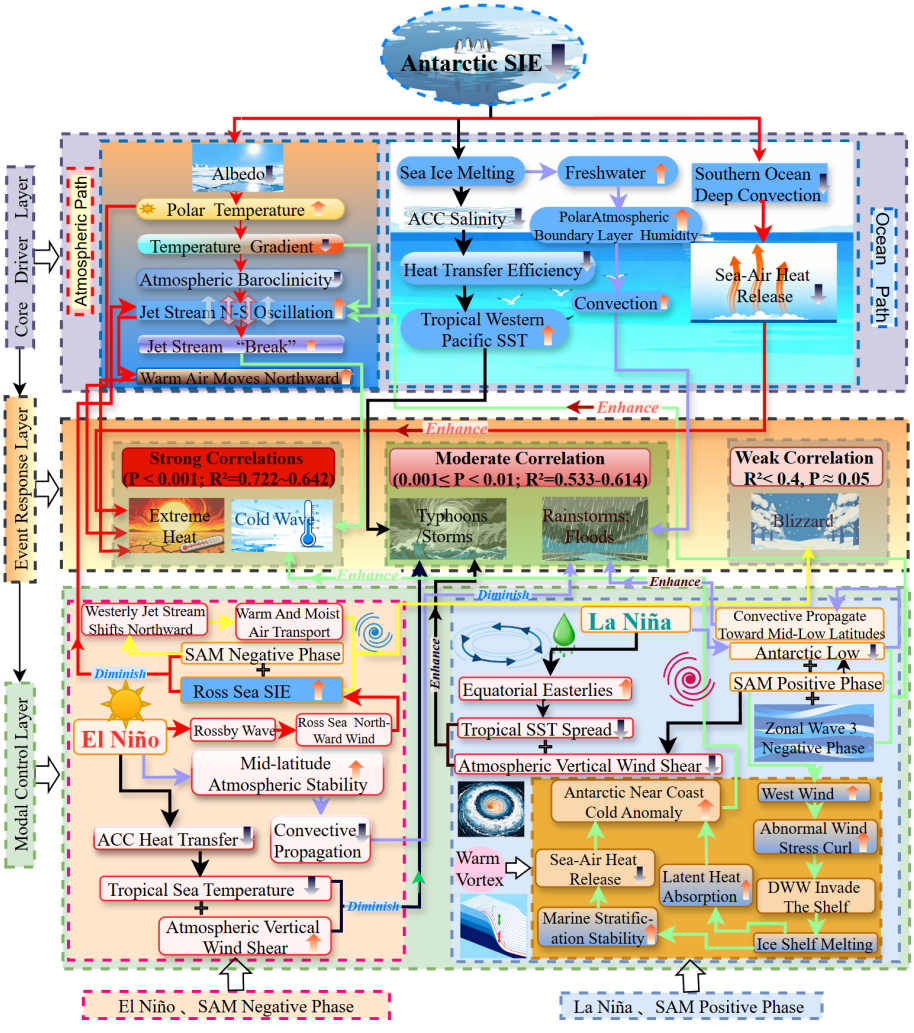

Figure 8: Schematic of Mechanism-Correlation Logic

Notes：This diagram illustrates the mechanism by which changes in Antarctic Sea Ice Extent (Antarctic SIE) affect multiple spheres of the climate system (such as the atmosphere and the ocean) and extreme weather events. Starting from the Core Driver Layer, through the Atmospheric path and the Ocean path, it acts on the Event Response Layer, and then at levels like the Modal Control Layer, it influences different extreme weather events such as extreme heat, cold waves, typhoons/storms, rainstorm/floods, and blizzards. It also involves the association with climate modes like El Niño and La Niña, reflecting the interaction relationships such as enhancement (Enhance) and diminishment (Diminish) among various factors and the strength of their correlations. Strong (red), medium (black), and weak (light green) logical lines of different colors point to their corresponding associated factors. The upward and downward arrows in each text box in the diagram are used to intuitively indicate the increasing or decreasing trends of relevant parameters, assisting in showing the changes in physical quantities and climatic elements (such as temperature, salinity, and circulation) in various spheres (such as the atmosphere and the ocean) caused by factors like changes in Antarctic sea ice extent, thereby clearly presenting the dynamic evolution and interaction relationships of quantities in each process.

https://doi.org/10.5194/egusphere-2025-6301
Preprint. Discussion started: 1 April 2026

Cold Wave: Antarctic sea ice retreat influences cold wave events through a chain mechanism of "reconfiguring temperature gradients — intensifying cold anomalies via warm vortex intrusion — ENSO and SAM locking cold air invasion pathways." In sea ice retreat zones (e.g., the Amundsen Sea), surface albedo differences cause spring warming of 0.53°C, while the East Antarctic ice sheet exhibits a delayed cold anomaly (temperature difference reaching 2.3°C). Together, these factors reduce the temperature gradient in the mid-to-high latitudes of the Southern Hemisphere by 0.6–0.8°C, resulting in a 40% increase in jet stream "break" frequency (Chen et al., 2024) and opening pathways for cold air southward incursions. The four consecutive cold waves in East Antarctica during July–August 2023 (with a single-station minimum temperature of -68.7°C) synchronized with a 22% reduction in SIE in the Bellingshausen Sea.

Warm vortex feedback further amplified cold anomalies: SAM positive phases drove enhanced westerlies, generating anomalous wind stress curl that propelled circumpolar Deep Warm Water (DWW) (temperature +0.8°C) to invade the shelf as anticyclonic vortices (Gao et al., 2024). The warm vortex triggered ice shelf melting; the latent heat absorbed during ice shelf melting can directly offset part of the heat transported by warm eddies, thereby mitigating the warming effect of these eddies on local water temperatures (Josey et al., 2018), and the freshwater influx from this melting increased ocean stratification stability by 25%. This, in turn, suppressed heat release from the ocean to the atmosphere, intensifying the Antarctic coastal cold anomaly (Jeromson et al., 2024**;** Kusahara et al., 2020). The occurrence of the coldest record in the Ross Sea in 2023 was directly related to a 37% increase in the frequency of warm vortex intrusions (Gao et al., 2024).

Climate modes significantly modulate cold waves: La Niña locks cold air into southward pathways via teleconnections (primarily affecting southern South America and southeastern Australia), while SAM in combination with the negative phase of Zonal Wave 3 shortens the jet oscillation period to 14 days, prolonging cold wave duration by 30% (Eabry et al., 2024), establishing a strong correlation between cold waves and sea ice changes ($R^2 = 0.642–0.643$, $p < 0.01$). Conversely, El Niño weakens polar cold anomalies (reducing temperature differences by 1.2°C), while the negative SAM phase stabilizes the westerly jet stream, ultimately reducing cold wave frequency by 40% (Wang et al., 2025).

Typhoons / Storms: Antarctic sea ice retreat influences tropical sea surface temperatures via the ACC, with ENSO and SAM further modulating typhoon generation conditions. Freshwater released from melting sea ice reduces ACC salinity, decreasing its heat transport efficiency by 8% per decade (Ma et al., 2020). This leads to elevated sea surface temperatures in the tropical western Pacific—reaching +1.5°C anomalies in 2023 when sea ice reached record lows (Josey et al., 2024)—meeting the thermal threshold for typhoon formation (SST ≥ 26.5°C). This increase contributed to a 40% rise in typhoon/storm frequency compared to the long-term average, aligning with the 400% increase in SIE decline observed in this study. The correlation between these two factors exhibits an $R^2 = 0.614$ ($P < 0.001$).

Climate modes exerted significant regulatory effects: La Niña intensified equatorial easterlies, hindering the spread of warm tropical sea surface temperatures（SST）, while positive SAM suppressed atmospheric vertical wind shear (days with shear < 10 m/s increased by 50%). The combined effect drove typhoon frequency to its peak during the 2021–2023 "triple La Niña" period. Conversely, El Niño weakened ACC heat transport and lowered tropical sea surface temperatures, while the negative

https://doi.org/10.5194/egusphere-2025-6301
Preprint. Discussion started: 1 April 2026

SAM phase increased vertical wind shear. This resulted in typhoon frequencies during the 2014–2016 El Niño period being 30% lower than those during La Niña years.

Rainstorm/ Flooding: Rainstormand flooding exhibit a moderate "convective-modal coupling" association with sea ice changes. The mechanism involves freshwater released from sea ice melt increasing polar atmospheric boundary layer humidity by 10%–15% (Komatsu et al., 2025), thereby stimulating localized convective activity. A positive SAM phase deepens the Antarctic Low (reducing central pressure by 3 hPa), propelling convective systems toward mid-to-low latitudes (with propagation speeds increasing by 20%). During 2010–2024, a 10% reduction in Antarctic sea ice correlates with an 8–12% increase in rainstormfrequency at mid-to-low latitudes (Zhu et al., 2023), yielding an $R^2 = 0.562$ ($P < 0.01$) for flood events linked to sea ice changes.

ENSO phase significantly influences correlation strength: El Niño enhances atmospheric stability in mid-to-low latitudes (Richardson number increases by 0.2), suppressing convective propagation; La Niña concentrates precipitation toward the tropics (precipitation share increases by 30%); only during ENSO neutral phases can positive SAM phases drive uniform convective transport (Okumura, 2019), peaking rainstormand flood frequency (e.g., 2018–2019). During the 2021–2023 “triple La Niña” period, synergistic effects between sea ice retreat and climate modes amplified rainstormfrequency increases by 20% compared to El Niño years (Figure 5).

Blizzards: Blizzards show a weak correlation with sea ice changes, with the core mechanism being a localized adaptation of “El Niño-induced localized sea ice accumulation + SAM negative phase conveying warm and moist airflows.” The global-scale correlation weakens: El Niño excites Ross Sea waves, strengthening northward winds in the Ross Sea region (wind speed increase of 1.0 m/s), driving sea ice accumulation toward the coast. During El Niño years from 2010 to 2024, the Ross Sea SIE increased by 5%–8% compared to normal years (Zhang et al., 2021), forming the “cold subsurface” conditions required for blizzards (days with temperatures < −25°C increased by 25%). The negative SAM phase shifts the westerly jet stream northward by 1.5 latitudes, conveying warm, moist air (relative humidity > 80%) from the Southern Ocean to the Ross Ice Shelf margin. The convergence of cold lower-level air and warm, moist air triggers a "convergence-upward–cooling–sublimation" process (upward velocity: 0.5 m/s). For instance, during the 2022 El Niño + negative SAM phase, heavy snowfall days in the Ross Sea increased by 25% (Zhang et al., 2024).

Weak correlation stems from two factors: first, this mechanism is confined to the Ross Sea region and opposes the “sea ice retreat-driven” mechanism observed during other extreme events; second, ENSO causes uneven snowstorm distribution—concentrated only in the Antarctic Peninsula and Ross Sea—and global-scale data smooth out local signals, ultimately yielding an $R^2 < 0.4$ ($P \approx 0.05$) (Hrudya et al., 2020). This study observes a “stabilization followed by decline” pattern in Antarctic SIE from 2010 to 2024, inconsistent with the slight increase observed from 1979 to 2010 (Parkinson, 2019). This discrepancy stems from the synergistic effects of the “triple La Niña” (Wang et al., 2025) and human-induced subsurface upwelling of warm water in the Southern Ocean (0.12°C/decade), adding to the emerging understanding that “short-term extreme climate modes accelerate sea ice retreat.” The conclusion of a “strong negative correlation between sea ice and heatwaves” in this paper aligns with Zhu et al. (2023). For cold waves, it proposes a three-dimensional mechanism involving the “temperature gradient–warm vortex–climate mode,” overcoming the limitation of existing studies that

https://doi.org/10.5194/egusphere-2025-6301
Preprint. Discussion started: 1 April 2026

focus solely on albedo. For heavy snow events, it quantifies, for the first time, the localized regulatory effect of "El Niño + negative SAM phase," providing a physical explanation for weakly correlated events.

4 Conclusion

Based on sea ice data from NSIDC for 2010–2024, global major disaster weather and climate event data from the China National Climate Center, and the El Niño–Southern Oscillation (ENSO) index, this study systematically analyzes the spatiotemporal evolution of Antarctic SIE, its association with ENSO, and the mechanisms through which it influences global extreme climate events. Antarctic SIE exhibits a pattern of "initial stability followed by decline + regional differentiation": From 2010 to 2014, fluctuations were minimal (±0.3 million km²). It peaked in September 2014 (20.16 million km²), then rapidly retreated after 2015, dropping to 1.85 million km² in February 2023 (a 20% decrease compared to the 2010–2014 summer average). Spatially, the Amundsen Sea–Bellingshausen Sea and Antarctic Peninsula form the core retreat zone. From 2020 to 2024, winter and summer sea ice concentrations in this region decreased by 10%–15% and 20%–25%, respectively, compared to the 2010–2019 period. This pattern contrasts sharply with the slight increase observed during 1979–2010 (Parkinson, 2019), stemming from the synergistic effects of the "triple La Niña" (Wang et al., 2025) and the upwelling of warm water in the subsurface layer of the Southern Ocean (0.12°C/decade) since 2016, complementing the understanding that "short-term extreme climate modes accelerate sea ice retreat."

Antarctic SIE variations are closely linked to ENSO: During El Niño years (2010, 2013–2015), both the North Equatorial Pacific Index (NEPI) and North Equatorial Counter Current Index (NCPI) exceeded 0, resulting in positive SIE anomalies. The Ross Sea SIE increased by 8%–10% due to Rossby wave teleconnections. During La Niña years (2011, 2017–2018, 2021–2023), both indices and SIE anomalies were negative, with the most pronounced negative anomalies occurring during the "triple La Niña" period. ENSO drives differential sea ice changes by regulating Antarctic wind fields and heat flux.

Global extreme weather events exhibit a "strong-moderate-weak" negative correlation with Antarctic sea ice, jointly regulated by ENSO and the SAM. Extreme heatwaves ($R^2 = 0.722$) and cold waves ($R^2 = 0.642$) exhibit strong correlations ($P < 0.001$), driven by the "albedo-circulation positive feedback" mechanism — sea ice retreat reduces albedo from 0.8 to 0.1; each 10% decrease in SIE increases polar solar radiation absorption by 15%–20%, leading to local warming of 2–3°C per decade, narrowing the mid-to-high latitude temperature gradient in the Southern Hemisphere (0.6–0.8°C), and widening the westerly jet oscillation (±1.2° to ±2.0°). The "strong negative correlation between sea ice and heatwaves" aligns with Zhu et al. (2023), while the cold wave mechanism involving the "temperature gradient–warm vortex–mode" overcomes existing limitations focused solely on albedo.

Floods ($R^2 = 0.562$), rainstorm($R^2 = 0.533$), and typhoons/storms ($R^2 = 0.614$) showed moderate associations ($0.001 \leq P < 0.01$), dependent on the "sea ice–ocean circulation–convection pathway": Sea ice meltwater reduces ACC salinity, decreasing heat transport efficiency by 8% per decade, leading to a +1.5°C tropical western Pacific sea surface temperature anomaly in 2023 (reaching the typhoon formation threshold); sea ice melt increases polar boundary layer humidity by 10%–15%, while the

https://doi.org/10.5194/egusphere-2025-6301
Preprint. Discussion started: 1 April 2026

positive SAM phase accelerates convective propagation toward mid-to-low latitudes by 20%.

Heavy snowfall ($R^2 < 0.4$, $P \approx 0.05$) shows a weak correlation, with only the Ross Sea exhibiting significant local effects: El Niño increases SIE in this region by 5%–8% (forming a cold subsurface layer < −25°C), while negative SAM phases shift the westerly jet northward by 1.5 latitudes, conveying warm, moist air (humidity > 80%) from the Southern Ocean to generate blizzards. Global data exhibit weakened correlations due to event clustering and signal smoothing; this study is the first to quantify the regulatory effect of the "El Niño + negative SAM phase" interaction. La Niña + positive SAM increased extreme heat frequency by 400% during 2021–2023, while El Niño suppressed this association. Study limitations: The 15-year data span is shorter than the climate system's 30-year cycle, necessitating integration of NSIDC data since 1979; global data lack resolution near Antarctica, requiring CRU data to optimize spatial detail; Arctic sea ice and greenhouse gases are excluded, demanding a multi-factor framework to quantify sea ice's potential 35%–40% contribution.

Author Contribution

Conceptualization: S. Tang & Y. Zang developed the research framework on Antarctic sea ice-global extreme weather links, defining 3 core objectives.
Data Curation: S. Tang collected/organized 2010–2024 NSIDC, CMA, NOAA data, verified consistency, and standardized formats.
Formal Analysis: Y. Zang did spatiotemporal decomposition of sea ice, exponential regression for event correlations, and significance testing.
Investigation: S. Tang validated key points via 2023 low sea ice/2021–2023 La Niña data and literature cross-checks.
Methodology: S. Tang built the "observation-simulation-mechanism" framework and optimized data analysis methods.
Writing - Original Draft: S. Tang structured chapters and organized core results.
Writing - Review & Editing: Y. Zang revised the manuscript, optimizing logic and adding citations.
Supervision: Both supervised the research, guiding analysis direction and approving the final version.
Validation: Both cross-checked sea ice analysis, correlation calculations, and mechanism inferences.

Acknowledgments

This study thanks the **U.S. National Snow and Ice Data Center (NSIDC)** for providing 2010–2024 Antarctic SIE and SIC data, which enabled analyzing sea ice's spatiotemporal evolution and core retreat zones. Gratitude also goes to the **China National Climate Centre (CNCC)** for its 2010–2024 global hazardous weather dataset, supporting quantification of sea ice-extreme event correlations. We acknowledge the U.S. NOAA/NCEP for GODAS-derived ENSO indices (NEPI, NCPI), vital for exploring climate mode impacts. Finally, thanks to Longdong University's School of Geography and Planning and Qingyang Tech Innovation Center for academic support.

References

https://doi.org/10.5194/egusphere-2025-6301
Preprint. Discussion started: 1 April 2026

1. Ayres, H. C., Screen, J. A., Blockley, E. W., & Bracegirdle, T. J. (2022). The coupled atmosphere-ocean response to Antarctic sea ice loss. *Journal of Climate, 35*(14), 4665–4685. https://doi.org/10.1175/jcli-d-21-0918.1
2. Bader, J., Flügge, M., Kvamsto, N. G., Mesquita, M. D. S., & Voigt, A. (2012). Atmospheric winter response to a projected future Antarctic sea-ice reduction: A dynamical analysis. *Climate Dynamics, 40*(11–12), 2707–2718. https://doi.org/10.1007/s00382-012-1507-9
3. Behringer, D. W., & Xue, Y. (2004). Evaluation of the global ocean data assimilation system at NCEP: The Pacific Ocean. In Eighth Symposium on Integrated Observing and Assimilation Systems for Atmosphere, Oceans, and Land Surface, AMS 84th Annual Meeting (pp. 11–15). Washington State Convention and Trade Center, Seattle, Washington.
4. Chen, H. B., & Cui, X. Y. (2024). *Polar Climate Change Annual Report (2023)*. China Meteorological Administration. https://www.cma.gov.cn/2011xwzx/2011xmtjj/202409/t20240909_6560216.html
5. Chen, X. M., Sharma, A., & Liu, H. (2023). The impact of climate change on environmental sustainability and human mortality. *Environments, 10*(10), 165. https://doi.org/10.3390/environments10100165
6. Cordero, R. R., et al. (2023). Signature of the stratosphere-troposphere coupling on recent record-breaking Antarctic sea-ice anomalies. *The Cryosphere, 17*(12), 4995–5006. https://doi.org/10.5194/tc-17-4995-2023
7. Crosta, X., et al. (2021). Multi-decadal trends in Antarctic sea-ice extent driven by ENSO-SAM over the last 2,000 years. *Nature Geoscience, 14*(3), 156–160. https://doi.org/10.1038/s41561-020-00666-7
8. Cvijanovic, I., & Caldeira, K. (2015). Antarctic sea ice and climate sensitivity. *Environmental Research Letters, 10*(9), 094011. https://doi.org/10.1088/1748-9326/10/9/094011
9. Cvijanovic, I., & Caldeira, K. (2015). Atmospheric impacts of sea ice decline in CO2 induced global warming. *Climate Dynamics, 44*(5–6), 1173–1186. https://doi.org/10.1007/s00382-015-2489-1
10. Dash, M. K., Pandey, P. C., Vyas, N. K., & Turner, J. (2012). Variability in the ENSO-induced southern hemispheric circulation and Antarctic SIE. *International Journal of Climatology, 33*(3), 778–783. https://doi.org/10.1002/joc.3456
11. Diamond, R., et al. (2024). CMIP6 models rarely simulate Antarctic winter sea-ice anomalies as large as observed in 2023. *Geophysical Research Letters, 51*(4), e2024GL109265. https://doi.org/10.1029/2024GL109265
12. Dou, J., & Zhang, R. (2022). Weakened relationship between ENSO and Antarctic sea ice in recent decades. *Climate Dynamics, 60*(5–6), 1313–1327. https://doi.org/10.1038/s41612-025-01066-0
13. Dou, X., & Zhang, S. (2022). ENSO impacts on Antarctic sea ice: A review. *Advances in Atmospheric Sciences, 39*(1), 2–22. https://doi.org/10.1007/s00376-021-1211-8
14. Eabry, M. D., Goyal, R., Taschetto, A. S., Hobbs, W., & Sen Gupta, A. (2024). Combined impacts of Southern Annular Mode and Zonal Wave 3 on Antarctic sea ice variability. *Journal of Climate, 37*(5), 1759–1775. https://doi.org/10.1175/JCLI-D-23-0516.1
15. Fetterer, F., Knowles, K., Meier, W. N., Savoie, M., & Windnagel, A. K. (2017). Sea Ice Index, Version 3 [Data set]. National Snow and Ice Data Center. Updated 2024. https://doi.org/10.7265/N5K072F8
16. Gao, L., Yuan, X., Cai, W., Guo, G., Yu, W., Shi, J., Qiao, F., Wei, Z., & Williams, G. D. (2024). Persistent warm-eddy transport to Antarctic ice shelves driven by enhanced summer westerlies. *Nature Communications, 15*(1), 671. https://doi.org/10.1038/s41467-024-45010-x
17. Gurjao, C. D., Pezzi, L. P., Parise, C. K., Justino, F. B., Carpenedo, C. B., Schumacher, V., & Comin, A. (2025). Atmospheric variability and sea-ice changes in the Southern Hemisphere. *Atmosphere, 16*(3), 284. https://doi.org/10.3390/atmos16030284
18. He, Y., Ding, X., Huang, J., Li, D., & Guan, X. (2019). The extreme cold winter under global warming. In AGU Fall Meeting Abstracts (Vol. 2019, GC51P-1060). American Geophysical Union.
19. Heuzé, C. (2021). Antarctic bottom water and North Atlantic deep water in CMIP6 models. *Ocean Science, 17*(1), 59–90. https://doi.org/10.5194/os-17-59-2021

https://doi.org/10.5194/egusphere-2025-6301
Preprint. Discussion started: 1 April 2026

20. Hrudya, S., Goswami, B., & Xavier, P. K. (2020). ENSO-driven variability in Antarctic sea ice and its impact on Indian summer monsoon rainfall. *International Journal of Climatology, 40*(15), 7163–7178. https://doi.org/10.1002/joc.6644
21. Jeromson, M. R., et al. (2024). Circumpolar Deep Water upwelling is a primary source of 10Be in Antarctic continental shelf sediments. *Global and Planetary Change, 236*, 104424. https://doi.org/10.1016/j.gloplacha.2024.104424
22. Jha, R., et al. (2025). Extreme terrestrial heat in 2024. *Nature Reviews Earth & Environment, 6*(4), 234–236. https://doi.org/10.1038/s43017-025-00661-2
23. Ji, D., et al. (2023). Global amplification of extreme heatwaves by surface solar radiation. *Nature Communications, 14*(1), 7065. https://doi.org/10.1038/s41467-023-42816-4
24. Ji, L., & Fan, K. (2023). Extreme heat waves in June 2021 over Europe regulated by shrinking Eurasian snow cover in mid-high latitudes. *Atmospheric Research, 295*, 107049. https://doi.org/10.1016/j.atmosres.2023.107049
25. Josey, S. A., Hirschi, J. J.-M., Sinha, B., Duchez, A., Grist, J. P., & Marsh, R. (2018). The Recent Atlantic Cold Anomaly: Causes, Consequences, and Related Phenomena. *Annual Review of Marine Science, 10*(1), 475–501. https://doi.org/10.1146/annurev-marine-121916-063102
26. Josey, S. A., et al. (2024). Record-low Antarctic sea ice in 2023 increased ocean heat loss and storms. *Nature, 636*(7985), 635–639. https://doi.org/10.1038/s41586-025-08118-5
27. Kusahara, K. (2020). Interannual-to-Multidecadal Responses of Antarctic Ice Shelf–Ocean Interaction and Coastal Water Masses during the Twentieth Century and the Early Twenty-First Century to Dynamic and Thermodynamic Forcing. *Journal of Climate, 33*(12), 4941–4973. https://doi.org/10.1175/jcli-d-19-0659.1
28. Komatsu, K., et al. (2025). Antarctic sea ice loss amplifies polar boundary layer convection. *Journal of Geophysical Research: Atmospheres, 130*(2), e2024JD039876. https://doi.org/10.1029/2024JD039876
29. Komatsu, M., Ohshima, K. I., Mensah, V., & Nakata, K. (2025). Mapping of sea-ice melting and net freshwater flux by sea-ice in the Southern Ocean. *Communications Earth & Environment, 6*(1). https://doi.org/10.1038/s43247-025-02560-2
30. Ma, L., Wang, B., & Cao, J. (2020). Impacts of atmosphere-sea ice-ocean interaction on Southern Ocean deep convection in a climate system model. *Climate Dynamics, 54*(9–10), 4075–4093. https://doi.org/10.1007/s00382-020-05218-1
31. Ma, X., et al. (2020). Antarctic sea ice control on the Southern Ocean meridional heat transport. *Geophysical Research Letters, 47*(18), e2020GL089025. https://doi.org/10.1029/2020GL089025
32. Morioka, Y., et al. (2024). Antarctic sea ice multidecadal variability triggered by Southern Annular Mode and deep convection. *Communications Earth & Environment, 5*(1), 633. https://doi.org/10.1038/s43247-024-01783-z
33. National Climate Center. (2024). Global extreme weather events statistics (2010–2024). https://cmdp.ncc-cma.net/Monitoring/cn_global_extreme.php
34. Okumura, Y. M. (2019). ENSO diversity from an atmospheric perspective. *Current Climate Change Reports, 5*(3), 245–257. https://doi.org/10.1007/s40641-019-00138-7
35. Osborne, M. R. (2010). *Finite algorithms in optimization and data analysis*. Society for Industrial and Applied Mathematics.
36. Parkinson, C. L. (2019). A 40-y record reveals gradual Antarctic sea ice increases followed by decreases at rates far exceeding the rates seen in the Arctic. *Proceedings of the National Academy of Sciences, 116*(30), 14414–14423. https://doi.org/10.1073/pnas.1900922116
37. Purich, A., & Doddridge, E. W. (2023). Record low Antarctic sea ice coverage indicates a new sea ice state. *Communications Earth & Environment, 4*(1), 314. https://doi.org/10.1038/s43247-023-00876-2
38. Rantanen, M., Räisänen, J., Sinclair, V. A., & Järvinen, H. (2018). Sensitivity of idealised baroclinic waves to mean atmospheric temperature and meridional temperature gradient changes. *Climate Dynamics, 52*(5–6), 2703–2719. https://doi.org/10.1007/s00382-018-4283-3

https://doi.org/10.5194/egusphere-2025-6301
Preprint. Discussion started: 1 April 2026

651 39. Rantanen, M., et al. (2018). Arctic amplification increases temperature variability in northern mid-latitudes.
652 *Nature Communications, 9*(1), 5144. https://doi.org/10.1038/s41467-018-07570-1
653 40. Tewari, K., Mishra, S. K., Salunke, P., et al. (2023). Potential effects of the projected Antarctic sea-ice loss on
654 the climate system. *Climate Dynamics, 60*, 589–601. https://doi.org/10.1007/s00382-022-06320-2
655 41. Wang, J., Luo, H., Yu, L., Li, X., Holland, P. R., & Yang, Q. (2023). The impacts of combined SAM and
656 ENSO on seasonal Antarctic sea ice changes. *Journal of Climate, 36*(11), 3553–3569.
657 https://doi.org/10.1175/jcli-d-22-0679.1
658 42. Wang, S., Liu, J., & Cai, W. (2025). Strong impact of the rare three-year La Niña event on Antarctic surface
659 climate changes in 2021–2023. *npj Climate and Atmospheric Science, 8*(1), 1–12.
660 https://doi.org/10.1038/s41612-025-01066-0
661 43. Zhang, C., Li, T., & Li, S. (2021). Impacts of CP- and EP-El Niño events on the Antarctic sea ice in austral
662 spring. *Journal of Climate, 34*(24), 10245–10260. https://doi.org/10.1175/JCLI-D-21-0002.1
663 44. Zhang, Y., Chen, H., & Cui, X. (2024). SAM negative phase and El Niño drive Antarctic blizzard under sea ice
664 accumulation. *The Cryosphere, 18*(5), 2101–2118. https://doi.org/10.5194/tc-18-2101-2024
665 45. Zhu, Z., Liu, J., Song, M., & Hu, Y. (2023). Changes in extreme temperature and precipitation over the
666 southern extratropical continents in response to Antarctic sea ice loss. *Journal of Climate, 36*(14), 4755–4775.
667 https://doi.org/10.1175/jcli-d-22-0577.1